International Journal of Pure and Applied Physics
Vol.2, No.1, pp.9-36, March 2014
Published by European Centre for Research Training and Development UK (www.ea-journals.org)

THE EFFECT OF RELATIVE HUMIDITY ON MARITIME POLLUTED AEROSOLS

B. I. Tijjani[1], F. Sha'aibu[2] and A. Aliyu[3]
[1]Department of Physics, Bayero University, Kano, NIGERIA
emails: idrith@yahoo.com , idrithtijjani@gmail.com
[2] Girl's Science and Technical College, Kano, Kano State, NIGERIA.
[3] Department of Science Laboratory Technology, School of Technology, Kano State Polytechnic, NIGERIA.

ABSTRACT: *In this paper, the author extracted and investigated the effect of relative humidity (RH) on some microphysical and optical properties of maritime polluted aerosols from OPAC at the spectral range of 0.25μm to 2.5μm and eight relative humidities (0, 50, 70, 80, 90, 95, 98, and 99%).The microphysical properties extracted were radii, volume mix ratio, number mix ratio and mass mix ratio as a function of RH while the optical properties were optical depth, extinction, scattering and absorption coefficients single scattering albedo, refractive indices and asymmetric parameters. Using the microphysical properties, hygroscopic growth factors and effective radii of the mixtures were determined while using optical properties we determined the enhancement parameters, effective refractive indices and Angstrom coefficients. The hygroscopic growth and enhancement parameters were then parameterized using some models to determine the hygroscopicity, bulk hygroscopicity, humidification factors and some other parameters that depend on RH and/or wavelengths. We observed that the data fitted the models very well. The effective radii increase with the increase in RH, while Angstrom coefficients decrease with the increase in RH and this signify the dominance of coarse mode particles. The angstrom coefficients show that the mixture has bimodal type of distribution and the mode size increases with the increase in RH.*

KEYWORDS: Microphysical Properties, Optical Properties, Hygroscopic Growth, Enhancement Parameters, Angstrom Coefficients, Effective Refractive Indices.

INTRODUCTION

The ability to predict the water content associated with aerosol particles is an important factor in reducing the uncertainties associated with climate change. The ambient relative humidity changes the microphysical and optical properties of hygroscopic atmospheric aerosols (Cheng et al., 2008), such as sea-salts and water solubles. These ambient atmospheric aerosols are external and internal mixtures of particles with different chemical compounds such as soot, sulphate, nitrate, organic carbon and mineral dust. The state of mixing of these components is crucial for understanding the role of aerosol particles in the atmosphere. In recent years, much attention has been paid to the mixing state of soot in aerosols (Jacobson, 2001; Moffet and Prather, 2009; Riemer et al., 2009, 2010; Zhang et al., 2008; Oshima et al., 2009), which influences the optical properties and climate effects of aerosols. As the ambient relative humidity (RH) changes, hygroscopic atmospheric aerosols can undergo phase transformation, droplet growth, and evaporation. Phase transformation

from a solid particle to a saline droplet usually occurs spontaneously when the RH reaches a level called the deliquescence humidity and its values depend also on the chemical composition of the aerosol particle (Orr et al. 1958, Tang 1976).Aerosol particles play an important role in the atmosphere, because they influence the radiative budget of the earth directly by scattering and absorbing the incoming sunlight and indirectly by serving as cloud condensation nuclei for the formation of fog and cloud droplets (Twomey, 1977). One of the important chemical aerosol properties that control the magnitude of this effect is their hygroscopicity as a result of the changes in RH. Depending on the chemical and physical compositions, aerosol particles can take up large amounts of water compared to their dry state as relative humidity increases to 100% and thus radically increase their sizes and change their optical properties

Hygroscopic properties of aerosol particles can be determined by their physical and chemical characteristics (Topping et al., 2005a, b). The Kohler equation is often used to describe both the hygroscopic growth and the activation of aerosol particles to cloud droplets, based on the aerosol's physicochemical properties (Kohler, 1936). However, these detailed properties are not always available for ambient aerosols. Size-dependent mixing states of various chemical compositions also increase the complexity. Recently, several single-parameter schemes have been proposed to simplify the Kohler equation. Hygroscopicity parameters such as κ and ρion have been defined as proxies of chemical composition to represent aerosol hygroscopic growth as well as the ability of aerosol particles to become cloud condensation nuclei (CCN) (Petters and Kreidenweis, 2007; Wex et al., 2007). Moreover, Rissler et al. (2010) recently overviewed several models which describe the aerosol hygroscopicity and the CCN activation. It is worth noting that the hygroscopicity parameter (κ or ρion) for the Kohler model is not always a constant with respect to RH, especially for the range of RH above 90%. Based on a review of observational data, Andreae and Rosenfeld (2008) suggested that continental and marine aerosols on average tend to cluster into relatively narrow ranges of effective hygroscopicity (continental $\kappa = 0.3\pm0.1$; marine $\kappa = 0.7\pm0.2$). Recent field studies are largely consistent with this view, but they show also systematic deviations for certain regions and conditions. For example, Gunthe et al. (2009) reported a characteristic value of $\kappa = 0.15$ for pristine tropical rainforest aerosols in central Amazonia, which are largely composed on secondary organic matter.Hygroscopic properties of aerosol particles were investigated in marine environments in several field studies in the last ten years (e.g., Berg et al., 1998; Swietlicki et al., 2000; Massling et al., 2003).

The main parameter used to characterize the hygroscopicity of the aerosol particles is the aerosol hygroscopic growth factor gf(RH), which is defined as the ratio of the particle diameter at any RH to the particle diameter at RH = 0 % (Kammermann et al., 2010; Swietlicki et al., 2008).Changes in the aerosol optical properties resulting from the particle hygroscopic growth are described by enhancement factors f (RH), which, for each optical parameter χ , are defined as the ratio between its values determined in any conditions χ (RH) and those determined in dry conditions χ (RH = 0 %). Technically, the enhancement factor for scattering and hemispherical backscattering can be determined for a chosen RH by using two nephelometers performing measurements at the chosen RH and in dry conditions (RH = 0 %), respectively (Pahlow et al., 2006; Kim et al., 2006; Schmidhauser et al., 2009; Fierz-Schmidhauser et al., 2010a–b; Zieger et al., 2011).

The aim of this study is to determine the aerosols hygroscopic growth and enhancement factors for maritime polluted aerosols from the data extracted from OPAC. One and two variables parameterizations models will be perform to determine the relationship of the particles' hygroscopic growth and enhancement parameters with the RH. Angstrom coefficients are used determine the particles' type and the type mode size distributions.

METHODOLOGY

The models extracted from OPAC are given in table 1.

Table 1 Compositions of aerosols types at 0% RH (Hess et al., 1998).

Components	**No. Con.(cm^{-3})**	**R_{min} (μm):**	**R_{max} (μm):**	**sigma:**	**R_{mod} (μm):**
water soluble	3,800.0000	0.0050	20.0000	2.2400	0.0212
soot	5,180.0000	0.0050	20.0000	2.0000	0.0118
Sea salt accumulation mode	20.0000	0.0050	20.0000	2.0300	0.2090
Sea salt coarse mode	0.0032	0.0050	60.0000	2.0300	1.7500

where water soluble components, consists of scattering aerosols, that are hygroscopic in nature, such as sulfates and nitrates present in anthropogenic pollution, soot, not soluble in water and therefore the particles are assumed not to grow with increasing relative humidity, Sea-salt accumulation and coarse modes are two kinds of salt contained in seawater that are more hygroscopic than water soluble.

The globally averaged direct aerosol Radiative forcing, ΔF_R, for absorbing aerosols was calculated using the equation derived by Chylek and Wong (1995)

$$\Delta F_R = -\frac{S_0}{4} T_{atm}^2 (1-N)\{(1-A)^2 2\beta\tau_{sca} - 4A\tau_{abs}\} \quad (1)$$

Where S_0 is a solar constant, T_{atm} is the transmittance of the atmosphere above the aerosol layer, N is the fraction of the sky covered by clouds, A is the albedo of underlying surface, β is the upscattering fraction of radiation scattered by aerosol into the atmosphere while τ_{sca} and τ_{abs} are the aerosol layer scattering and absorptions optical thickness respectively. The above expression gives the radiative forcing due to the change of reflectance of the earth-aerosol system. The upscattering fraction is calculated using an approximate relation (Sagan and Pollack, 1967)

$$\beta = \frac{1}{2}(1-g) \quad (2)$$

where g is the asymmetric parameter. The global averaged albedo A=0.22 over land and A=0.06 over the ocean with 80% of aerosols being over the land; solar constant of 1370Wm^{-2}, the atmospheric transmittance is taken to be T_{atm}=0.79 (Penner et al, 1992) and cloudness N=0.6.

The aerosol's hygroscopic growth factor gf(RH), (Swietlicki et al. , 2008; Randles, et al., 2004) is defined as:

$$gf(RH) = \frac{D(RH)}{D(RH=0)} \quad (3)$$

where RH is taken for seven values 50%, 70%, 80%, 90%, 95%, 98% and 99%.

But since atmospheric aerosols consist of more and less hygroscopic sub fractions so the information on the hygroscopicity modes was merged into an "over-all" or "bulk" hygroscopic growth factor of the mixture, $gf_{mix}(RH)$, representative for the entire particle population as:

$$gf_{mix}(RH) = (\sum_k x_k gf_k^3)^{1/3} \quad (4)$$

The effective or volume equivalent radius of the mixture was determined using the relation

$$r_{eff}(RH) = (\sum_k x_k r_k^3)^{1/3} \quad (5)$$

where the summation is performed over all compounds present in the particles and x_k represent their respective volume fractions, using the Zdanovskii-Stokes-Robinson relation (ZSR relation; Sjogren et al., 2007; Stokes and Robinson, 1966; Meyer et al., 2009; Stokes et al., 1966; Stock et al., 2011). Solute-solute interactions are neglected in this model and volume additivity is also assumed. The model assumes spherical particles, ideal mixing (i.e. no volume change upon mixing) and independent water uptake of the organic and inorganic components. It can also be computed using the x_k as the corresponding number fractions (Duplissy et al., 2011; Meier et al., 2009). We now proposed the x_k to represent the mass mix ratio of the individual particles.

The RH dependence of $gf_{mix}(RH)$ can be parameterized in a good approximation by a one-parameter equation, proposed e.g. by Petters and Kreidenweis(2007) as:

$$gf_{mix}(a_w) = \left(1 + \kappa \frac{a_w}{1-a_w}\right)^{\frac{1}{3}} \quad (6)$$

Here, a_w is the water activity, which can be replaced by the relative humidity RH, if the Kelvin effect is negligible, as for particles with sizes more relevant for light scattering and absorption. The coefficient κ is a simple measure of the particle's hygroscopicity and captures all solute properties (Raoult effect), that is, it is for the ensemble of the particle which can be defined in terms of the sum of its components. In an ensemble of aerosol particles, the hygroscopicity of each particle can be described by an "effective" hygroscopicity parameter κ (Petters and Kreidenweis, 2007; Sullivan et al., 2009). Here "effective" means that the parameter accounts not only for the reduction of water activity by the solute but also for surface tension effects (Rose et al., 2008; Gunthe et al., 2009; Poschl et al., 2009). It also scales the volume of water associated with a unit volume of dry particle (Petters and Kreidenweis, 2007) and depends on the molar volume and the activity coefficients of the dissolved compounds (Christensen and Petters, 2012). The κ value derived for a particle of a given composition may vary, depending upon the size molar mass, the activity and RH it is derived at.

For atmospheric aerosols, the range of κ typically varies from as low as ~0.01 for some combustion aerosol particles up to ~1 for sea-salt particles (Petters and Kreidenweis, 2007; Andreae and Rosenfeld, 2008; Niedermeier et al., 2008; Petters et al., 2009).

The following sub-divisions at 85% RH were made by Liu et al., 2011 and Swietlicki et al., (2008); as: nearly-hydrophobic particles (NH): $\kappa <= 0.10$ ($gf_{mix} <= 1.21$), less-hygroscopic particles (LH): $\kappa = 0.10 - 0.20$ ($gf_{mix} = 1.21 - 1.37$); more-hygroscopic particles (MH): $\kappa > 0.20$ ($gf_{mix} > 1.37$).

Making κ as the subject of the equation (6), we get

$$k(a_w) = \frac{[gf_{mix}^3(a_w) - 1](1-a_w)}{a_w} \quad (7)$$

Humidograms of the ambient aerosols obtained in various atmospheric conditions showed that $gf_{mix}(RH)$ could as well be fitted well with a γ-law (Swietlicki et al., 2000; Birmili et al., 2004; Kasten, 1969; Gysel et al., 2009; Putaud, 2012) as

$$gf_{mix}(RH) = (1 - RH)^{\gamma} \quad (8)$$

Making γ as the subject of equation (8) we get

$$\gamma(RH) = \frac{ln(gf_{mix}(RH))}{ln(1-RH)} \quad (9)$$

The bulk hygroscopicity factor B under subsaturation RH conditions was determined using the relation:

$$B = (1 - gf_{mix}^{3})lna_{w} \quad (10)$$

where a_w is the water activity, which can be replaced by the RH as explained before.

The impact of hygroscopic growth on the optical properties of aerosols is usually described by the enhancement factor $f_{\chi}(RH, \lambda)$:

$$f_{\chi}(RH, \lambda) = \frac{\chi(RH,\lambda)}{\chi(RH_{ref},\lambda)} \quad (11)$$

where in our study RH_{ref} was 0%, and RH was taken for seven values of 50%, 70%, 80%, 90%, 95%, 98% and 99%.

In general the relationship between $f_{\chi}(RH, \lambda)$ and RH is nonlinear (e.g. Jeong et al. 2007). In this paper we determine the empirical relations between the enhancement parameter and RH (Doherty et. al., 2005) as:

$$f_{\chi}(RH, \lambda) = \frac{\chi(RH,\lambda)}{\chi(RH_{ref},\lambda)} = \left(\frac{100-RH_{ref}}{100-RH}\right)^{\gamma} \quad (12)$$

The γ known as the humidification factor represents the dependence of aerosol optical properties on RH, which results from the changes in the particles sizes and refractive indices upon humidification. The use of γ has the advantage of describing the hygroscopic behavior of aerosols in a linear manner over a broad range of RH values; it also implies that particles are deliquesced (Quinn et al., 2005), a reasonable assumption for this data set due to the high ambient relative humidity during the field study. The γ parameter is dimensionless, and it increases with increasing particle water uptake.

Making γ as the subject of equation(12) and $RH_{ref} = 0$, we get

$$\gamma(RH, \lambda) = -\frac{ln\left(f_{\chi}(RH,\lambda)\right)}{ln(1-RH)} \quad (13)$$

From previous studies, typical values of γ for ambient aerosol ranged between 0.1 and 1.5 (Gasso et. al., 2000; Quinn et al., 2005; Clarke et al., 2007).

Two parameters empirical relation was also used (Jeong et. al., 2007; Hanel, (1976)) as;

$$f_{\chi}(RH, \lambda) = a(1 - RH)^{b} \quad (14)$$

Equations (12) and (14) were verified at wavelengths 0.25, 0.45, 0.55, 0.70, 1.25, and 2.50μm.

To determine the effect of particles distributions as a result of change in RH, the Angstrom exponent was determined using the spectral behavior of the aerosol optical depth, with the wavelength of light (λ) was expressed as inverse power law (Angstrom, 1961):

$$\tau(\lambda) = \beta\lambda^{-\alpha} \quad (15)$$

The Angstrom exponent was obtained as a coefficient of the following regression,

$$ln\,\tau(\lambda) = -\alpha ln(\lambda) + ln\beta \quad (16)$$

However equation (16) was determined as non-linear (that is the Angstrom exponent itself varies with wavelength), and a more precise empirical relationship between the optical depth and wavelength was obtained with a 2nd-order polynomial (King and Byrne, 1976; Eck et al., 1999; Eck. et al., 2001a, b,; Kaufman, 1993;O'Neill et al., 2001, 2003; Pedros et al, 2003; Kaskaoutis and Kambezidis, 2006; Schmid et al., 2003; Martinez-Lozano et al., 2001) as:

$$\ln\tau(\lambda)=\alpha_2(\ln\lambda)^2 + \alpha_1\ln\lambda + \ln\beta \quad (17)$$

and then we proposed the cubic relation to determine the type of mode distribution as:

$$\ln X(\lambda)= \ln\beta + \alpha_1\ln\lambda + \alpha_2(\ln\lambda)^2+ \alpha_3(\ln\lambda)^3 \quad (18)$$

where β, α, α_1, α_2, α_3 are constants that were determined using regression analysis with SPSS16.0. for wondows.

We also determined the exponential dependence of the aerosol optical thickness on relative humidity as done by Jeong et al. (2007) as;

$$\tau(RH) = Ae^{B(RH/100)} \quad (19)$$

where A and B are constants determined using regression analysis with SPSS 16.0 and was computed at wavelengths 0.25, 1.25 and 2.50μm.

We finally determine the effect of hygroscopic growth on the effective refractive indices of the mixed aerosols using the following formula (Aspens, 1982):

$$\frac{\varepsilon_{eff}-\varepsilon_0}{\varepsilon_{eff}+2\varepsilon_0} = \sum_i f_i \frac{\varepsilon_i-\varepsilon_0}{\varepsilon_i+2\varepsilon_0} \quad (20)$$

The relation between dielectrics and refractive indices is

$$m_i = \sqrt{\varepsilon_i} \quad (21)$$

We also used another mixing rule formula that has been used in the several widely employed databases of aerosol optical properties (Heller, 1945; Wang and Martin (2007); Shettle and Fenn, 1979; d'Almeida et al., 1991; Hess et al., 1998) as:

$$m = \sum_i f_i m_i \quad (22)$$

where f_i and ε_i are the volume fraction and dielectric constant of the i^{th} component and ε_0 is the dielectric constant of the host material. For the case of Lorentz-Lorentz (Lorentz, 1880; Lorentz, 1880), the host material is taken to be vacuum, ε_0 =1.

We then proposed the f_i to be mass mix ratios and number mix ratios, to determine the advantage of one over the other.

The computations of equations (20), (21) and (22) were done using the complex functions of Microsoft Excel 2010.

RESULTS AND DISCUSSIONS

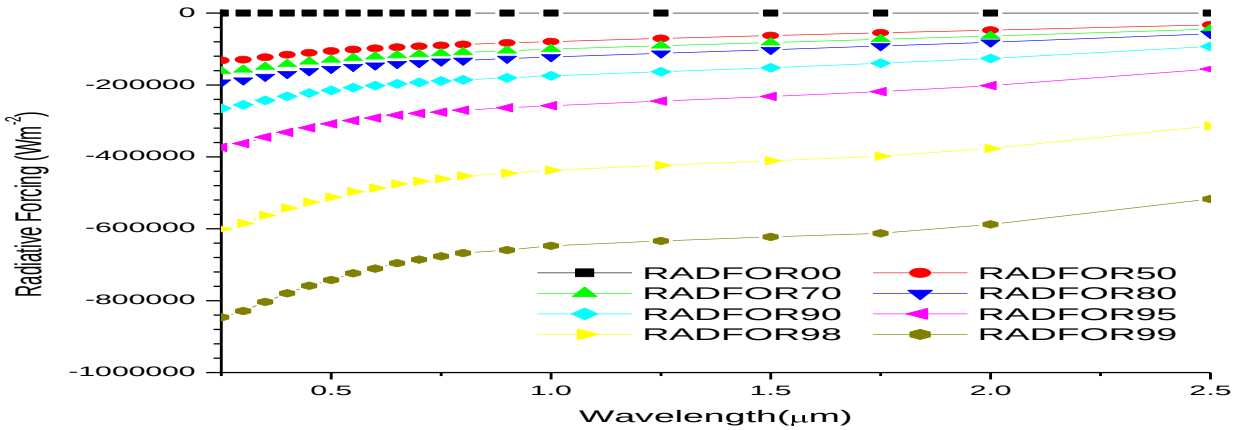

Figure 1: A graph of Radiative forcing against wavelengths

From figure 1, the RF at 0% RH is almost 0, with respect to wavelengths. But as the RH increases, the RF(cooling) also increases but the increase is more at shorter wavelength. The nature of the variations of the RF with RH and wavelengths at longer wavelengths shows the dominance of very hygroscopic and coarse particles.

Table 2: the table of hygroscopic growth factors, effective radii, B (bulk hygroscopicity), κ (hygroscopicity) and γ (Humidification factor), of the aerosols using number mix ratio.

RH(%)	0	50	70	80	90	95	98	99
gf_{mix}(RH) equ (4)	1.0000	1.1138	1.1731	1.2304	1.3522	1.5100	1.7628	1.9626
r_{eff} (μm) equ (5)	0.0301	0.0465	0.0522	0.0573	0.0682	0.0828	0.1092	0.1353
B equ (10)		0.2646	0.2191	0.1925	0.1551	0.1253	0.0905	0.0659
κ equ (7)		0.3818	0.2633	0.2156	0.1636	0.1286	0.0914	0.0663
γ equ(9)		-0.1555	-0.1326	-0.1288	-0.1310	-0.1376	-0.1449	-0.1464

From table 2, it can be observe that there are increases in gf_{mix},and r_{eff}, decreases in B and κ whileγ fluctuates with the changes in RH.

The results of the parameterizations by one parameter of equations (6) and (8) using number mix ratio are:

k=0.0737, R^2= 0.9497 from equation (6)

γ=-0.1420, R^2= 0.9982 from equation (8)

From the observations of R^2, it can be seen that the data fitted the equations very well.

Table 3: the table of hygroscopic growth factors, effective radii, B (bulk hygroscopicity), κ (hygroscopicity) and γ (Humidification factor), of the aerosols using volume mix ratio.

RH(%)	0	50	70	80	90	95	98	99
gf_{mix}(RH) equ (4)	1.0000	1.5598	1.7554	1.9332	2.3120	2.8193	3.7443	4.6648
r_{eff} (μm) equ (5)	0.5524	0.7616	0.8042	0.8381	0.9007	0.9699	1.0836	1.2040
B equ (10)		1.9371	1.5726	1.3892	1.1967	1.0982	1.0403	1.0101
κ equ (7)		2.7947	1.8895	1.5563	1.2620	1.1268	1.0509	1.0152
γ equ(9)		-0.6413	-0.4674	-0.4096	-0.3640	-0.3460	-0.3375	-0.3344

From table 3, it can be observe that there are increases in gf_{mix}, r_{eff} and γ, while there are decreases in B and κ with the changes in RH.

The results of the parameterizations by one parameter of equations (6) and (8) using volume mix ratio are:
k= 1.0279 , R^2= 0.9983 from equation (6)
γ= -0.3496 , R^2= 0.9885 from equation (8)

From the observations of R^2, it can be seen that the data fitted the equations very well.

Table 4: the table of hygroscopic growth factors, effective radii, B (bulk hygroscopicity), κ (hygroscopicity) and γ (Humidification factor), of the aerosols using mass mix ratio.

RH(%)	0	50	70	80	90	95	98	99
gf_{mix}(RH) equ (4)	1.0000	1.5564	1.7513	1.9286	2.3077	2.8149	3.7399	4.6604
r_{eff} (μm) equ (5)	0.5649	0.7575	0.8023	0.8357	0.8979	0.9675	1.0821	1.2019
B equ (10)		1.9202	1.5591	1.3775	1.1894	1.0927	1.0366	1.0073
κ equ (7)		2.7702	1.8734	1.5433	1.2543	1.1212	1.0471	1.0123
γ equ(9)		-0.6382	-0.4654	-0.4081	-0.3632	-0.3455	-0.3372	-0.3342

From table 4, it can be observe that there are increases in gf_{mix}, r_{eff} and γ, while there are decreases in B and κ with the changes in RH.

The results of the parameterizations by one parameter of equations (6) and (8) using mass mix ratio are:
k=1.0248, R^2= 0.9984 from equation (6)
γ=-0.3492, R^2= 0.9887 from equation (8)

From the observations of R^2, it can be seen that the data fitted the equations very well.

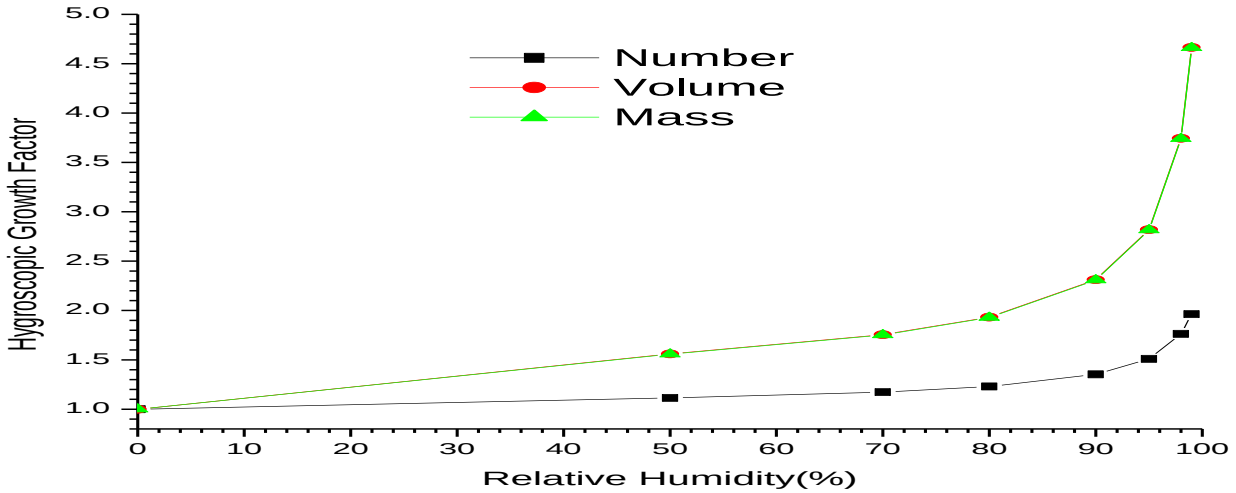

Figure 2: a graph of gf_{mix} against RH using number, volume and mass mix ratios using the data from tables (2), (3) and (4).

From figure 2 it can be observed that gf_{mix} using volume and mass mix ratios are the same, but has lower values using number mix ratios. All the plots satisfy power law.

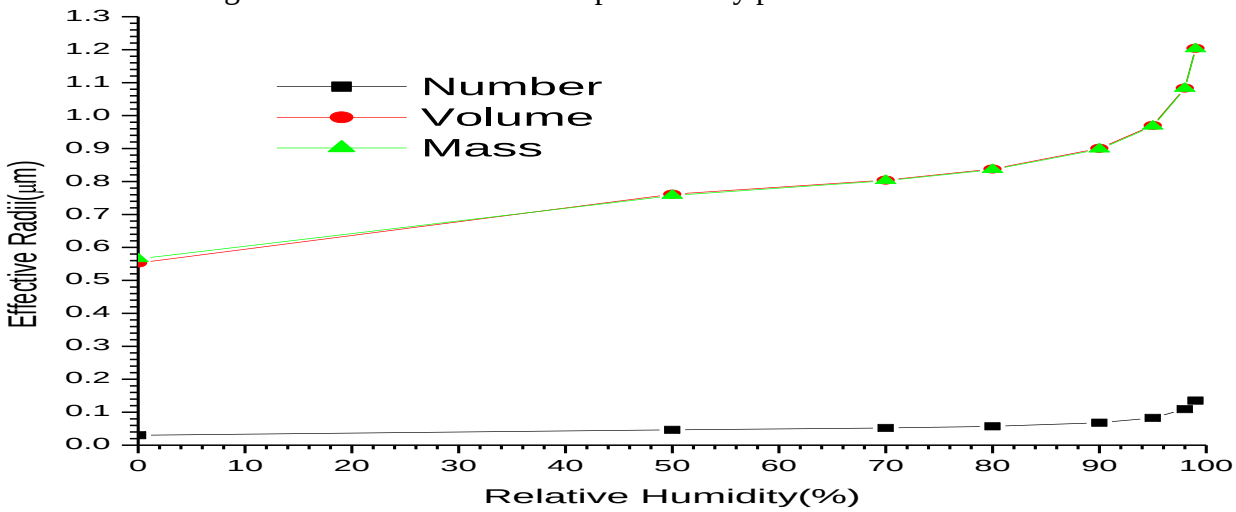

Figure 3: a graph of effective radii against RH using number, volume and mass mix ratios using the data from tables (2), (3) and (4).

Figure 3 shows that r_{eff} using volume and mass mix ratios are the same but number mix ratios has lower values It also shows that using volume and mass mix ratios, the r_{eff} increases faster with the increase in RHs, compared to number mix ratios. They also satisfy power law.

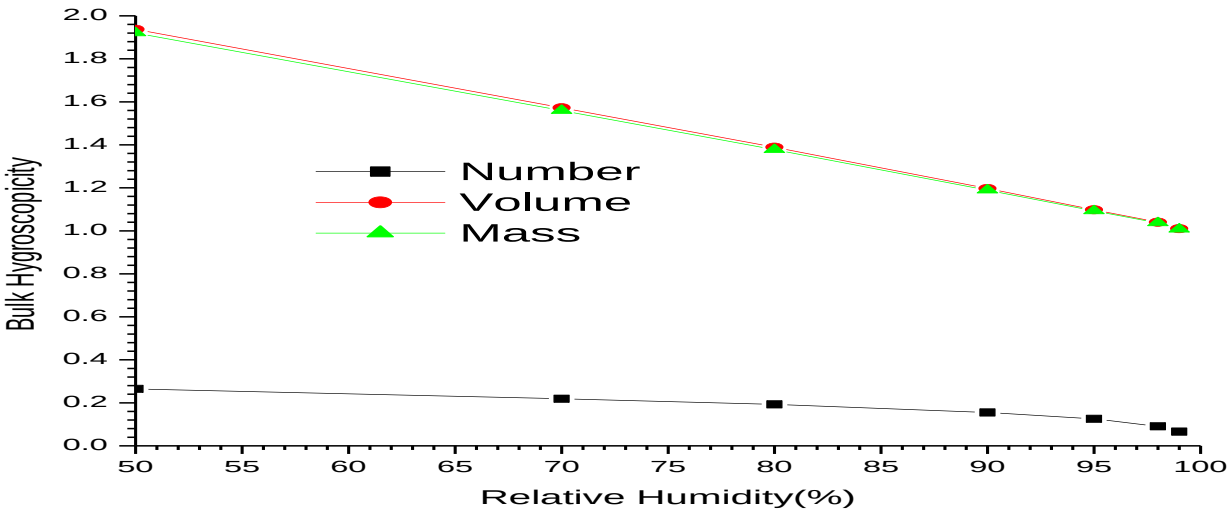

Figure 4: a graph of B (bulk hygroscopicity) against RH using number, volume and mass mix ratios using the data from tables (2), (3) and (4).

From figure 4, it can be seen that B has higher values using volume and mass mix ratios than number mix ratio, and decreases with the increase in RH in almost power law form.

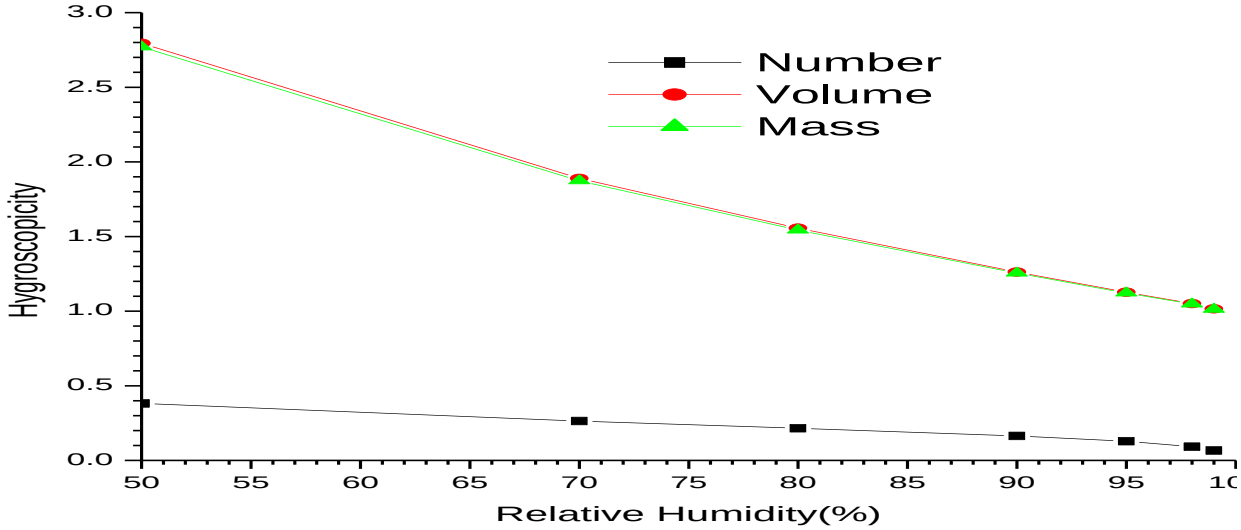

Figure 5: a graph of κ (hygroscopicity) against RH using number, volume and mass mix ratios using the data from tables (2), (3) and (4).

From figure 5, it can be seen that κ decreases with the increase in RH in a nonlinear form. It can also be observe that number mix ratio has the least while mass and volume mix ratio have the higher values.

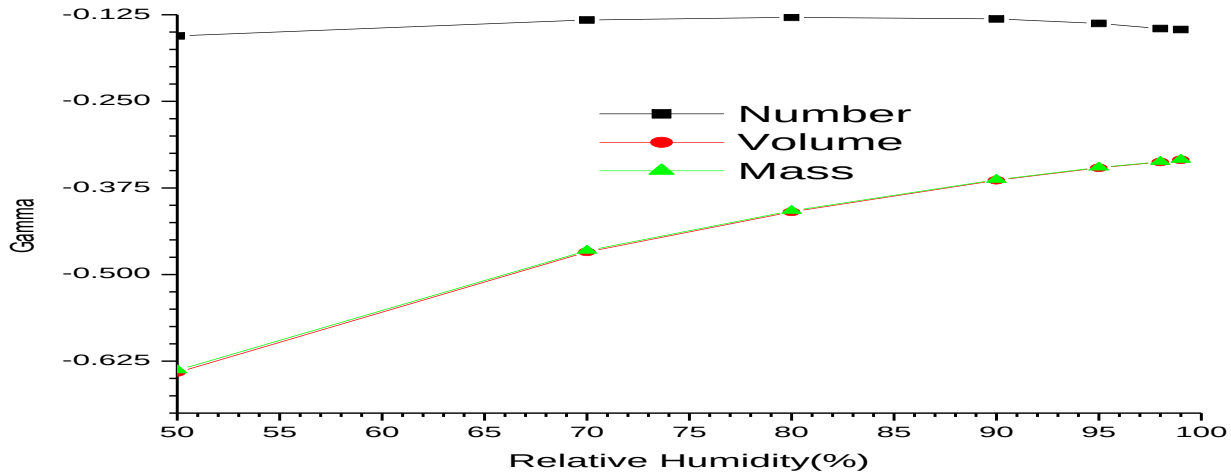

Figure 6: a graph of γ against RH using number, volume and mass mix ratios using the data from tables (2), (3) and (4).

From figure 6, it can be seen that γ has least in magnitude using number mix ratio, while it has the higher magnitude using volume and mass mix ratios.

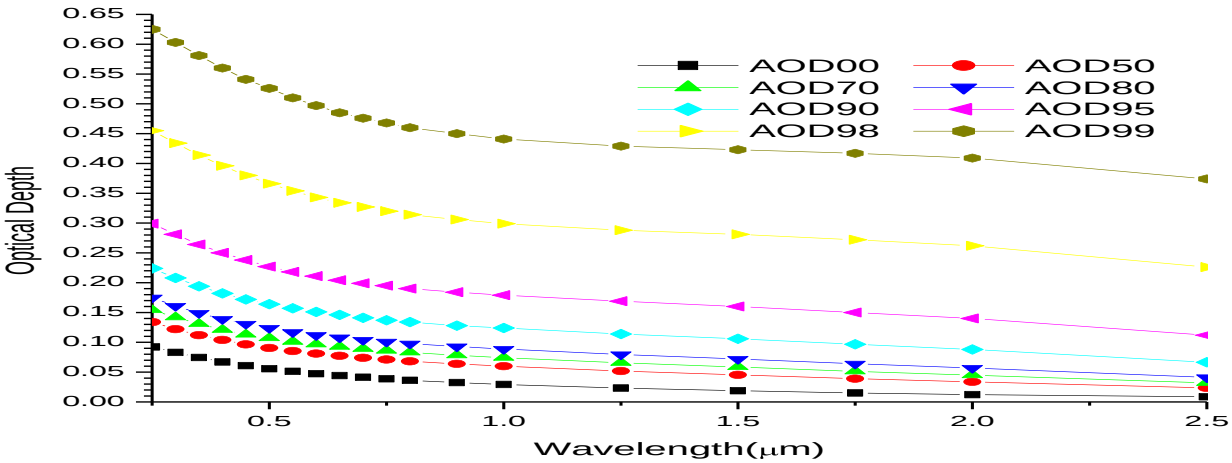

Figure 7: A graph of optical depth against wavelengths

From figure 7 as from 0% to 90% RH, the optical depth decreases monotonically with wavelengths and increases with the increase in the RH as a result of the hygroscopic growth. But as the RH increases from 95 to 99% RH the optical depth the monotonically behavior continue to decrease with respect to wavelength and RH. This behavior may be attributed to the dominance of coarse mode and very hygroscopic particles, which increases with the increase in RH. The behavior of the power law decreases with the increase in RHs, This also signifies the increase in the dominance of coarse particles with the increase in RH.

Using the data for plotting figure 7, the results of exponential relation between optical depth and RHs using equation (19) are:
At λ=0.25, A= 0.0706, B= 1.5866, R^2= 0.6955
At λ=1.25 μ, A= 0.0171, B= 2.4981, R^2= 0.7829

At λ=2.50 μ, A= 0.0057, B= 3.2321, R^2= 0.7906
The relation between optical depth and RH shows increase in R^2 and exponent B with the increase in wavelengths, and this signifies the dominance of coarse and very hygroscopic particles.

Table 5 *the results of the Angstrom coefficients for optical depth using equations (16), (17) and (18) at the respective relative humidities using regression analysis with SPSS16 for windows.*

RH	Linear		Quadratic			Cubic			
(%)	R^2	α	R^2	α1	α2	R^2	α1	α2	α3
0	0.9828	1.0064	0.9991	-1.0946	-0.1920	0.9997	-1.0553	-0.2369	-0.0588
50	0.9755	0.6905	0.9921	-0.7517	-0.1332	0.9980	-0.6623	-0.2351	-0.1336
70	0.9751	0.6167	0.9889	-0.6666	-0.1088	0.9969	-0.5737	-0.2148	-0.1390
80	0.9753	0.5610	0.9864	-0.6018	-0.0890	0.9959	-0.5100	-0.1937	-0.1373
90	0.9773	0.4658	0.9828	-0.4897	-0.0521	0.9938	-0.4076	-0.1458	-0.1228
95	0.9806	0.3777	0.9812	-0.3839	-0.0136	0.9914	-0.3201	-0.0864	-0.0954
98	0.9791	0.2773	0.9833	-0.2650	0.0269	0.9872	-0.2356	-0.0066	-0.0438
99	0.9684	0.2137	0.9871	-0.1935	0.0440	0.9873	-0.1883	0.0382	-0.0077

At 0% RH, the value of α is greater than 1, and this signifies the dominance of fine particles. But as the RH increases, it continues to decrease signifying the dominance of coarse and very hygroscopic particles. From the quadratic part, the negative curvature (α2) decreases with the increase in RH and become positive and increase further and this also signifies increase in the effective radii of the coarse particles with the increase in RH. This increase can be observed in tables (2), (3) and (4) where it can be seen that the effective radii increase with the increase in RHs. The cubic part signifies mode distributions as bi-modal.

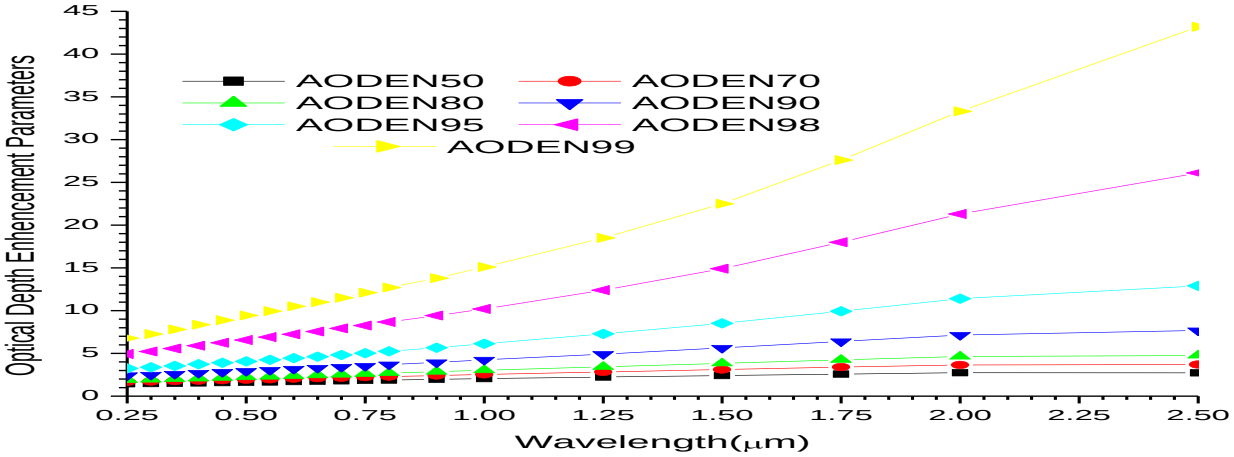

Figure 8: A graph of enhancement parameter for optical depth against wavelengths

Figure 8 shows that the enhancement factors increase with the increase in RH and wavelengths in almost power law form. One interesting phenomena is that at the near infrared region up to the infrared it can be seen that the enhancement is higher with the increase in RH and wavelengths. This signifies the dominance of coarse and very hygroscopic particles.

The results of the fitted curves of equations (12) and (14) using the data for plotting figure 8 are presented as follows;
For a single parameter using equation (12).
At λ=0.25μ, γ= 0.4076, R^2= 0.9984
At λ=0.45μ, γ= 0.4694, R^2= 0.9979
At λ=0.55 μ, γ= 0.4983, R^2= 0.9974
At λ=0.70 μ, γ= 0.5367, R^2= 0.9959
At λ=1.25 μ, γ= 0.6639, R^2= 0.9906
At λ=2.50 μ, γ= 0.8545, R^2= 0.9922
For two parameters using equation (14).
At λ=0.25μ, a= 1.0294, b= -0.3985, R^2= 0.9934
At λ=0.45μ, a= 1.0815, b= -0.4449, R^2= 0.9936
At λ=0.55 μ, a= 1.1197, b= -0.4629, R^2= 0.9941
At λ=0.70 μ, a= 1.2004, b= -0.4795, R^2= 0.9952
At λ=1.25 μ, a= 1.4594, b= -0.5455, R^2= 0.9983
At λ=2.50 μ, a= 1.5576, b= -0.7157, R^2= 0.9985

For both one and two parameters, the values of R^2 signify excellent relation and the increase in the exponents signifies increase in relation with wavelength. This signifies the dominance of coarse and very hygroscopic particles.

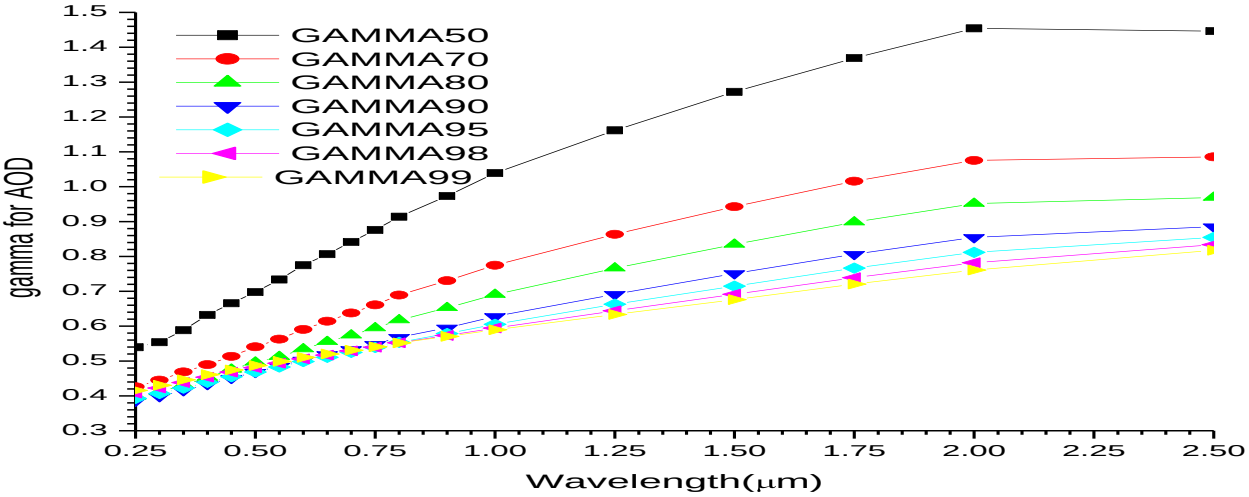

Figure 9 a graph of γ against wavelength using equation (13)

Figure 9 shows increase in γ with the increase in RHs and wavelengths, and the increase is more significant at higher RHs and wavelengths. This also signifies the dominance of coarse and very hygroscopic particles.

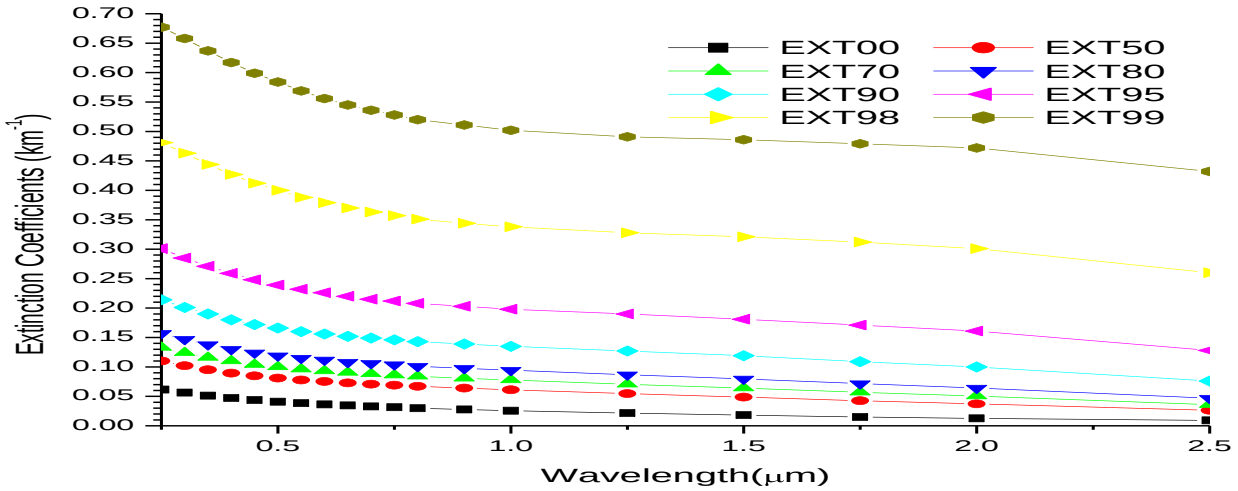

Figure 10: A graph of extinction coefficients against wavelengths

From figure 10, comparing figure 10 with 7, it can be observe that they are the same, with values of the plots in figure 10 having higher than those of figure 7.

Using the data for plotting figure 10, the results of exponential relation between extinction coefficient and RHs using equation (19) are:
At λ=0.25, A= 0.0461, B= 2.0425, R^2=0.7577
At λ=1.25 μ, A= 0.0160, B= 2.6992, R^2=0.7927
At λ=2.50 μ, A= 0.0060, B= 3.3224, R^2=0.8142
The relation between optical depth and RH shows increase in R^2 and exponent B with the increase in wavelengths, and this signifies the dominance of coarse and very hygroscopic particles.

Table 6 *the results of the Angstrom coefficients for extinction coefficient using equations (16), (17) and (18) at the respective relative humidities using regression analysis with SPSS16 for windows.*

RH	Linear		Quadratic			Cubic			
(%)	R2	α	R2	α1	α2	R2	α1	α2	α3
0	0.9744	0.7864	0.9965	-0.8670	-0.1754	0.9995	-0.7940	-0.2587	-0.1092
50	0.9490	0.5400	0.9813	-0.6077	-0.1475	0.9973	-0.4911	-0.2806	-0.1745
70	0.9478	0.4860	0.9766	-0.5438	-0.1257	0.9958	-0.4292	-0.2565	-0.1714
80	0.9500	0.4471	0.9739	-0.4954	-0.1051	0.9948	-0.3854	-0.2306	-0.1645
90	0.9561	0.3792	0.9699	-0.4103	-0.0676	0.9924	-0.3136	-0.1779	-0.1446
95	0.9661	0.3152	0.9691	-0.3272	-0.0260	0.9877	-0.2546	-0.1088	-0.1085
98	0.9738	0.2374	0.9761	-0.2296	0.0170	0.9836	-0.1949	-0.0225	-0.0518
99	0.9663	0.1845	0.9833	-0.1678	0.0363	0.9839	-0.1602	0.0277	-0.0113

From table 6, at 0% RH, the value of α is less than 1, and this signifies the dominance of coarse particles. The remaining observations are the same as those in table (5).

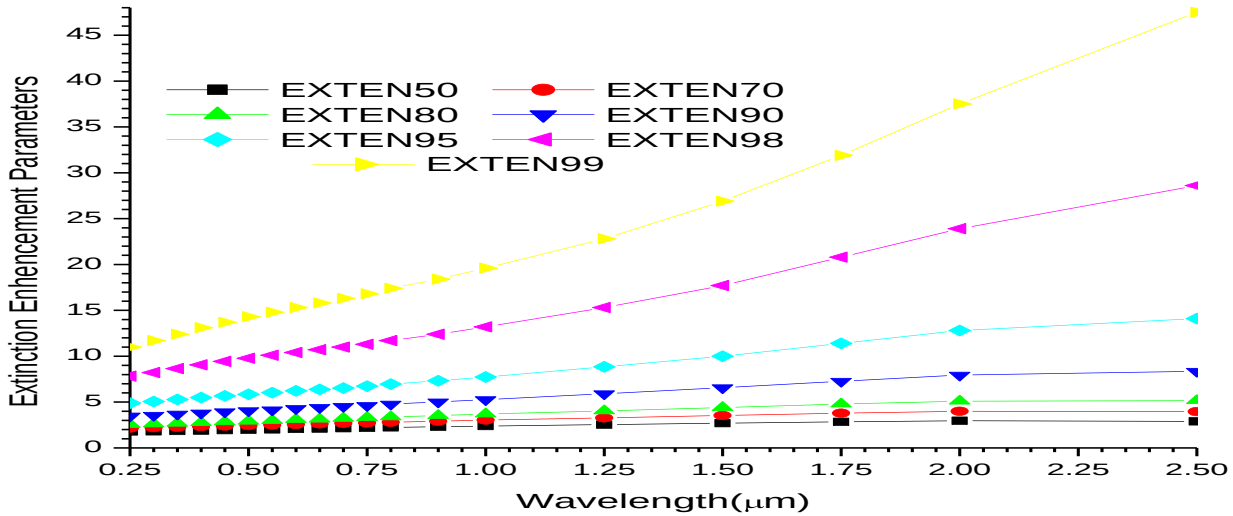

Figure 11: A graph of enhancement parameter for extinction coefficients against wavelengths

From figure 11, comparing figure 11 with 8, it can be observe that they are the same, with values of the plots in figure 11 having higher than those of figure 8.

The results of the fitted curves of equations (12) and (14) using the data for plotting figure 11 are presented as follows;

For a single parameter using equation (12),

At λ=0.25μ, γ= 0.5350, R^2= 0.9955

At λ=0.45μ, γ= 0.5853, R^2= 0.9942

At λ=0.55 μ, γ= 0.6045 , R^2= 0.9930

At λ=0.70 μ, γ= 0.6318, R^2= 0.9909

At λ=1.25 μ, γ= 0.7235, R^2= 0.9860

At λ=2.50 μ, γ= 0.8807, R^2= 0.9905

For two parameters using equation (14),

At λ=0.25μ, a= 1.2262, b= -0.4712, R^2= 0.9978

At λ=0.45μ, a= 1.2907, b= -0.5054, R^2= 0.9972

At λ=0.55 μ, a= 1.3381, b= -0.5132, R^2= 0.9973

At λ=0.70 μ, a= 1.4228, b= -0.5214, R^2= 0.9978

At λ=1.25 μ, a= 1.6628, b= -0.5643, R^2= 0.9992

At λ=2.50 μ, a= 1.6570, b= -0.7225, R^2= 0.9988

For both one and two parameters, the values of R^2 signify excellent relation and the increase in the exponents signifies increase in relation with wavelength. This also signifies the dominance of coarse and very hygroscopic particles.

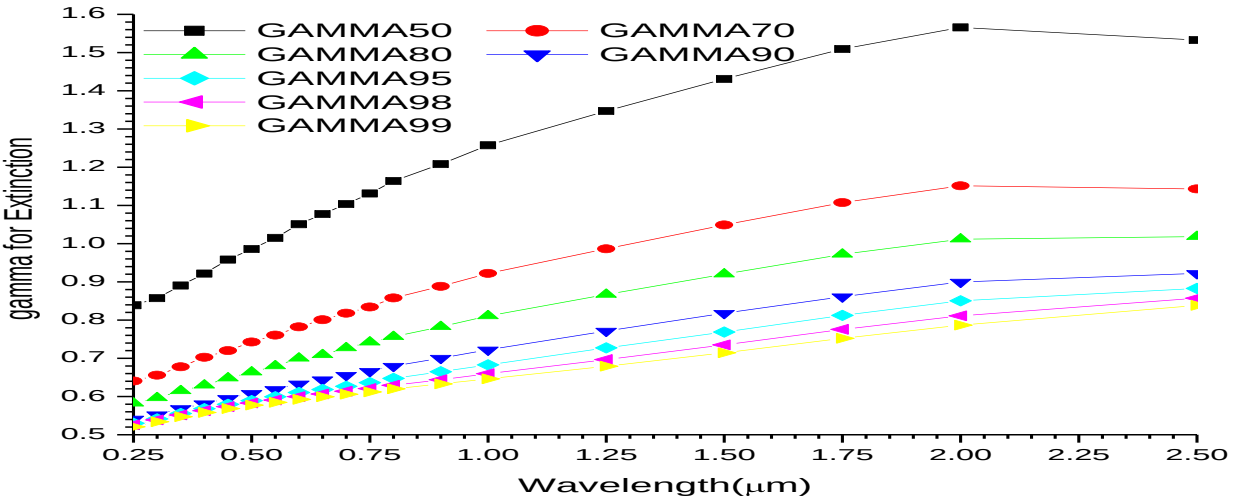

Figure 12: a graph of γ against wavelengths using equation (13).

Figure 12 is similar to figure 9, but γ for figure 12 is higher than that of figure 9 and more sparsely separated.

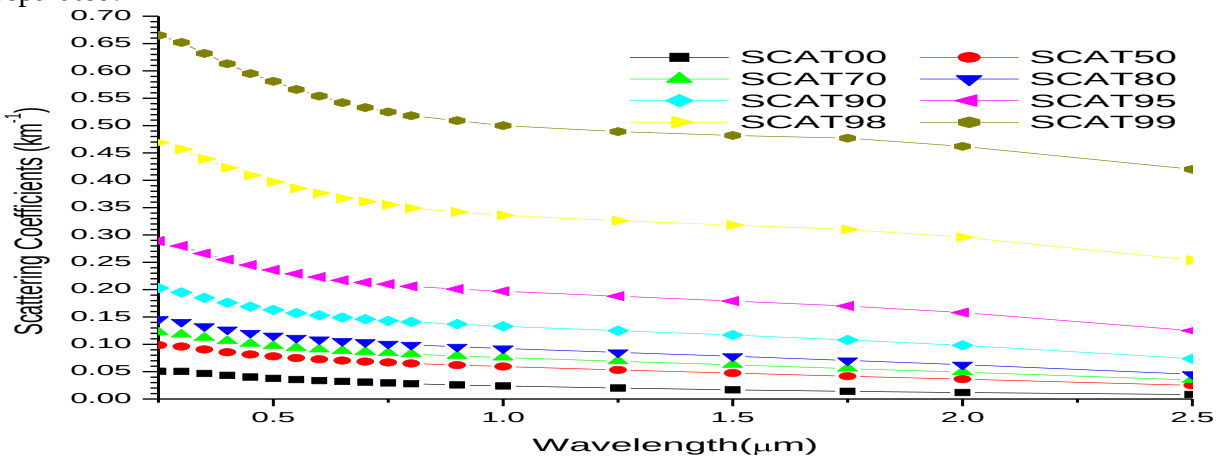

Figure 13: A graph of scattering coefficients against wavelengths

From figure 13, comparing figure 13 with figures 10 and 7, it can be observe that they are similar.

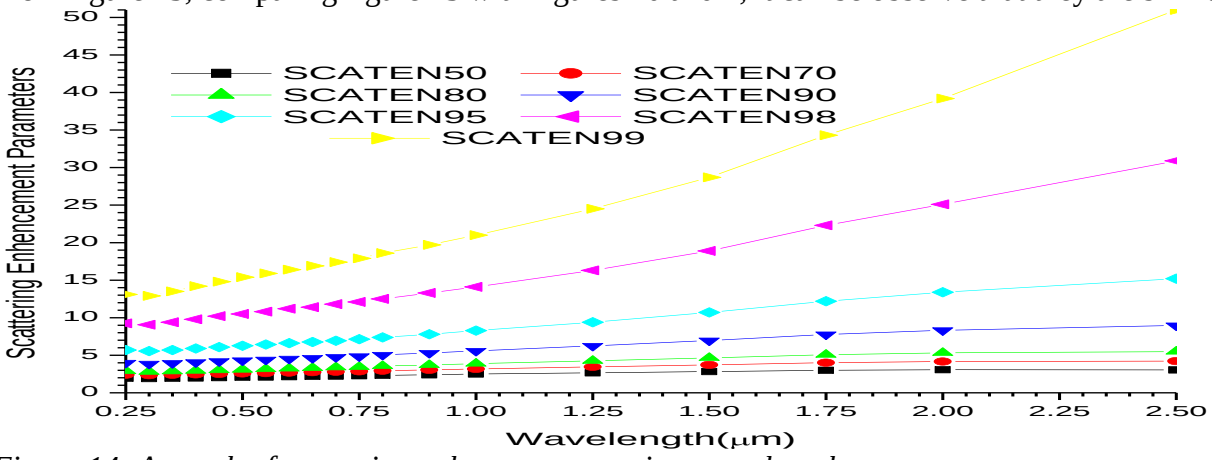

Figure 14: A graph of scattering enhancement against wavelengths

From figure 14, comparing figure 14 with figures 11 and 8, it can be observe that they are similar.

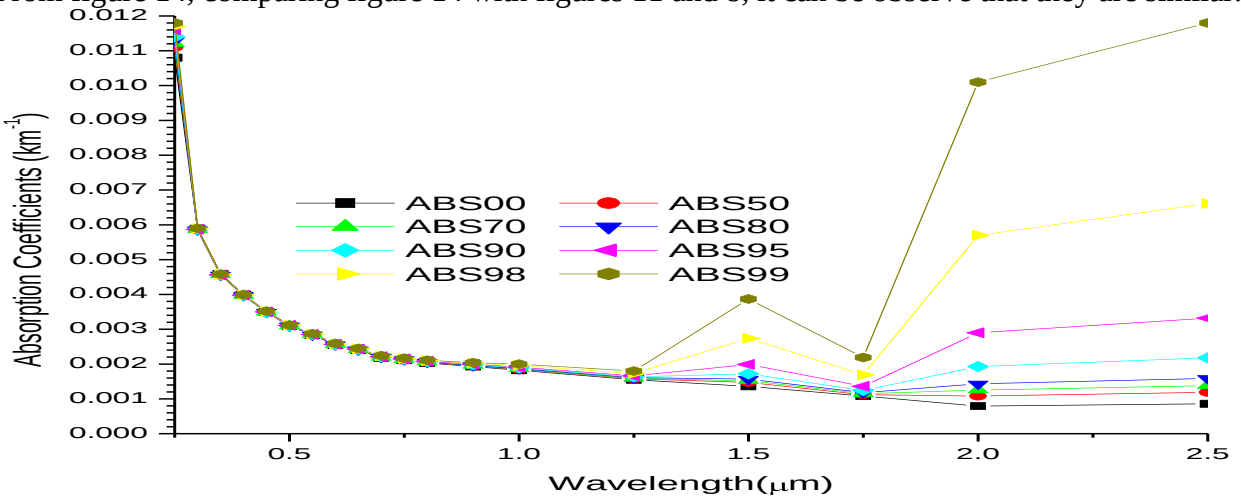

Figure 15: A graph of absorption coefficients against wavelengths

From figure 15, it can be seen that the absorption coefficients decreases monotonically with the increase in wavelengths at the spectral interval of 0.25 to 1.25μm and is almost independent of RHs. But at higher wavelengths the monotonical behavior continues up to approximately 80% RH, but after that, it became non monotonical and increase more with the increase in wavelengths and RHs. It also shows that power law can be obeyed only at 0 to 80% RHs. This signifies the dominance of coarse particles.

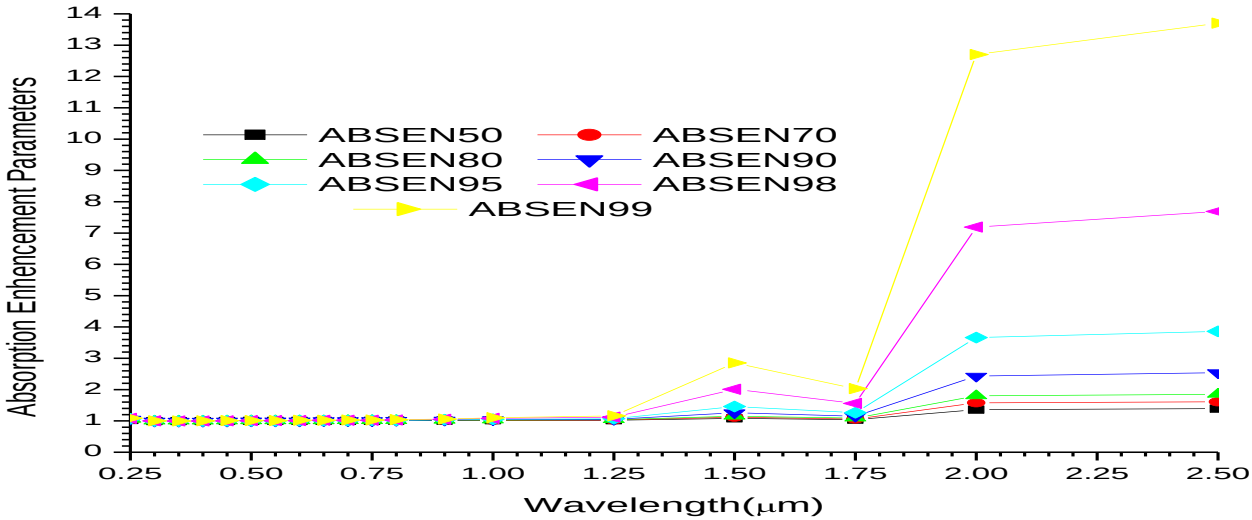

Figure 16: A graph of absorption enhancement against wavelengths

Figure 16 shows that it is almost 1 as from 0.25μm to 1.25μm and is independent of RH, but as from 1.25μm it increases with the increase in wavelength and RHs in a non-linear form. This shows the dominance of coarse particles.

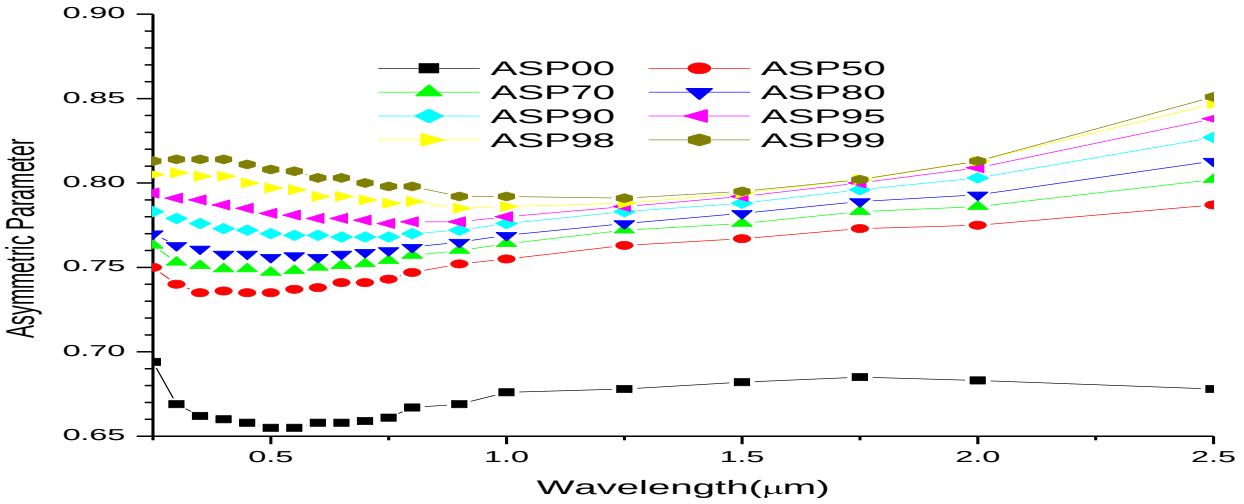

Figure 17: A graph of Asymmetric parameter against wavelengths

Figure 17 shows that hygroscopic growth has caused increase in scattering in the forward direction especially at shorter wavelength and longer wavelengths. Its relation with wavelengths and RH is non-linear. This can be attributed to high hygroscopicity of these aerosols particles and probably due to internal mixing.

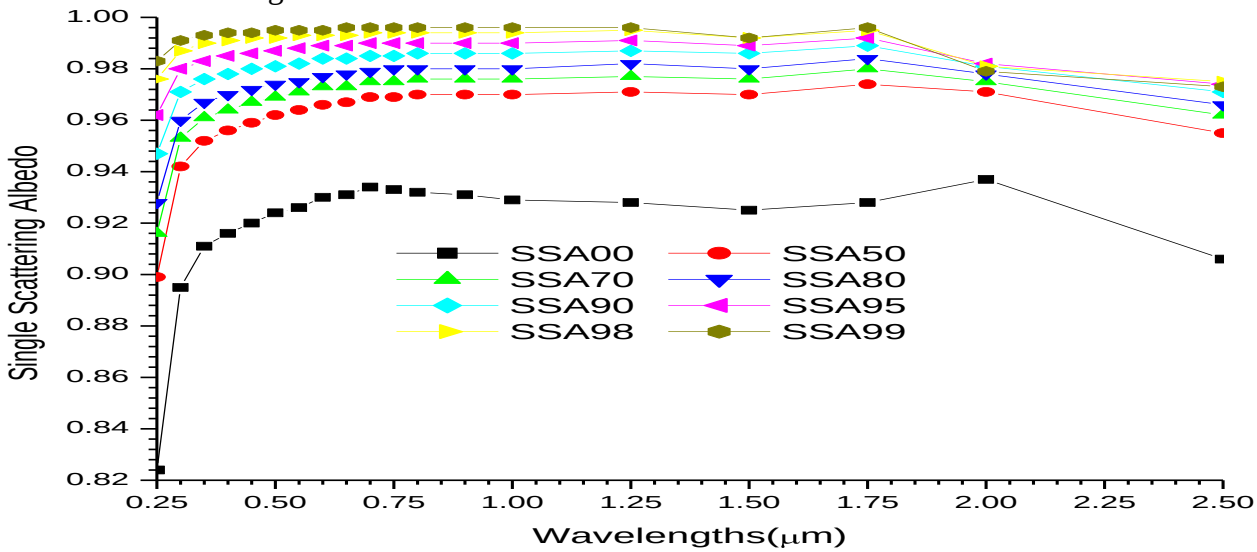

Figure 18: A graph of Single Scattering albedo against wavelengths

From figure 18, it can be observe that the plots are non-linear between single scattering albedo with RH and wavelengths. It also shows that as the RH increases, scattering became more dominant at shorter wavelengths while at larger wavelengths, absorptions increases with wavelengths. This is in line with was observed in figure 15.

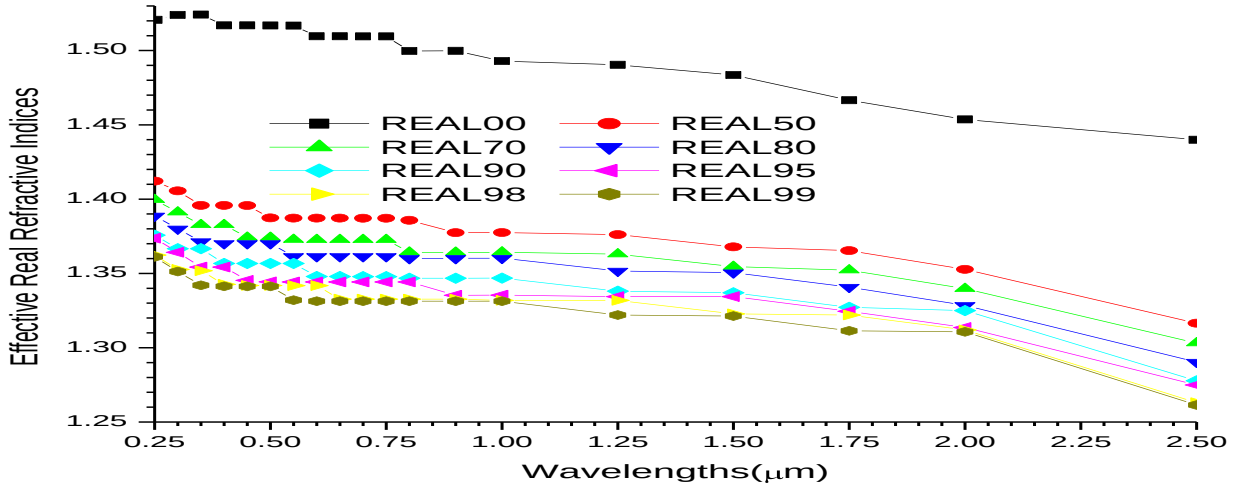

Figure 19: A plot of real effective refractive indices against wavelength using equation 20.

Figure 19, the non-liner relationship between the real effective refractive indices and wavelengths at 0% RH signifies the dominance of coarse particles. But as the RH increases, its behaviors with respect to wavelengths and RHs show that the mixtures are internally mixed, probably, because all the particles are very hygroscopic. Also, probably because the hygroscopic particles are acting as cloud condensation nuclei to soot, that is why its presence is not shown.

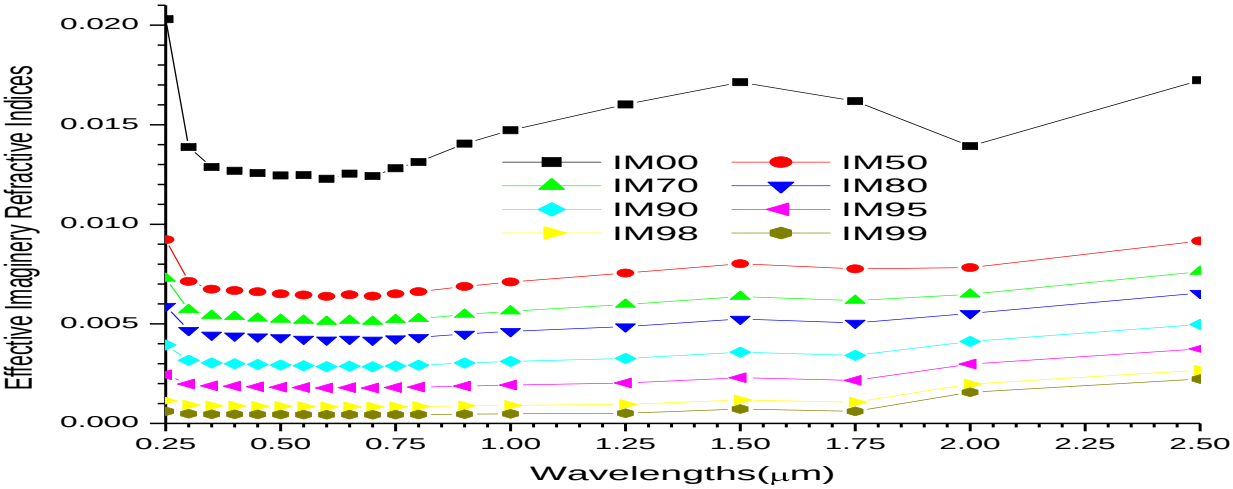

Figure 20: A plot of imaginary effective refractive indices against wavelength using equation 20.

Figure 20 shows that hygroscopic growth causes decrease in the imaginary refractive indices with the increase in RH. It behavior with wavelength at 0% RH signifies the dominance of coarse particles, but as the RH increase it can be observe that change to the extent that the plots are becoming more at the spectral interval of 0.3 to 1.25. The behaviors of the plots with respect to wavelength and RH as the RH increases shows that the mixture may be externally mix with respect to effective imaginary refractive indices, because of the presence of soot which is not soluble in water and has higher imaginary refractive indices.

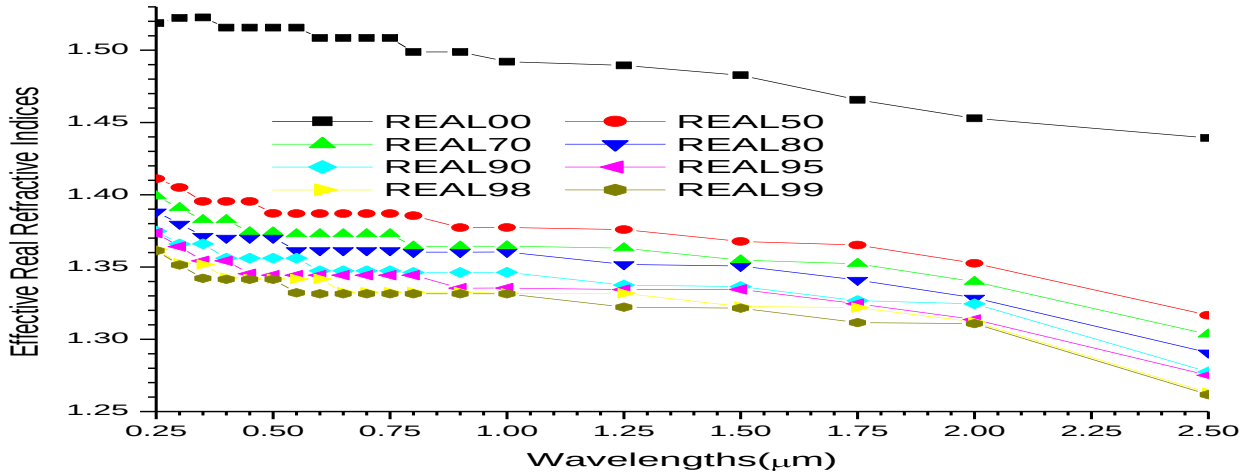

Figure 21: A plot of real effective refractive indices against wavelength using equation 22.

From figure 21, comparing figure 21 with 19, it can be seen that they are similar.

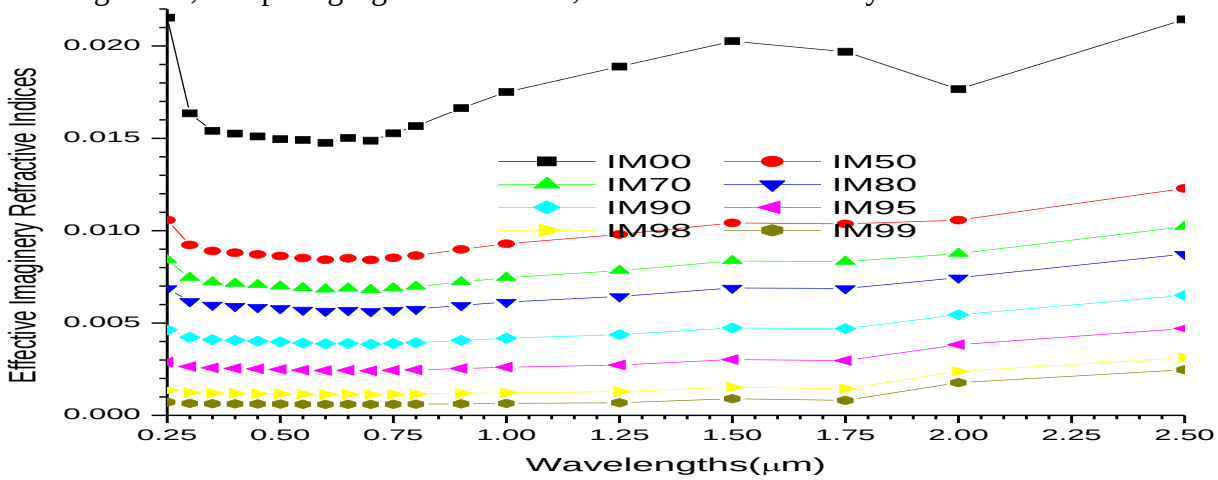

Figure 22: A plot of imaginary effective refractive indices against wavelength using equation 22.
From figure 22, comparing figure 22 with 21, it can be seen that they are similar.

CONCLUSIONS

Comparing the three types of gf_{mix} obtained, it can be seen that using volume and mass mix ratios gave better representations of the mixture. These also imply that optical effects of atmospheric aerosols are also more closely related to their volume than their number (Whitby, 1978; Seinfeld and Pandis , 1998). From the magnitude of the $gf_{mix}(RH)$ observed, it is assumed that the high number fraction of water soluble and sea salt accumulation mode is responsible for its high value. The relations between optical and microphysical properties with RH are such that at the deliquescence point (95 to 99%) this growth with higher humidities increases substantially, making this process strongly nonlinear with relative humidity (Fitzgerald, 1975; Tang, 1996; Kuś mierczyk-Michulec, 2009).

The characteristics of hygroscopic growth together with the asymmetric parameters show that smaller particles and very hygroscopic coarse particles reveal an immense potential of light

scattering enhancement in the forward scattering and the potential for the coarse and very hygroscopic particles of being highly effective cloud condensation nuclei. It also shows that the mixture is internally mixed for coarse particles because of the nature of the increase in scattering as a result of the hygroscopic growth (Wang and Martin, 2007) and the increase in absorption despite decrease in effective imaginary refractive indices. Therefore, the behavior of internal mixing and the relative importance of the humidity dependences of particle size and index of refraction on the aerosol scattering coefficient for a given substance depends on RH and on the sizes of the particles that provide the dominant contribution to the scattering.

Despite the excellent relation shown for k and γ using equations (6) and (8), but by observing their values using equations (7) and (9) in tables (2), (3) and (4), it can be observed that the values of these parameters in equation (6) and (8) could seriously underestimate those of equation (7) and (8) most especially at lower RHs. Therefore, based on these observations and the observations of hygroscopic parameters in tables (2), (3) and (4), show that all of hygroscopic parameters are always dependent on RH. The modeling of gf_{mix} with equations (6) and (8) show excellent relation because of the values of R^2, and all converge to 1 as the RH or a_w approach 0. The values of R^2 for equation (6) is always less than that of equation (8), and this may be attributed to the kelvin effect of equation (6) which was neglected.

From the modeling of the enhancement parameters using equations (12) and (14), it can be observe that there is a very excellent relation. However, based on convergence the convergence behavior of the two models as RH approaches 0, it can be seen that equation (12) is better, because at this limit it approaches 1, which is what it is supposed to be.

Jeong et al. (2007) demonstrated an exponential dependence of the aerosol optical thickness on relative humidity. The behavior of exponential relation between optical depth and extinction coefficients with RH, show that it is sensitive to the change in the effective radii and depends on the particles that provide the dominant contribution to scattering.

The decrease in the Angstrom coefficients in a non-linear form and the decrease in curvature with RH is in line with the increase in the effective radii with the increase in RH. As a consequence of such a non-uniform increase, the Ångström coefficient also becomes a function of RH. The observed variations in Angstrom coefficients can be explained by changes in the effective radii of the mixture resulting from changes in RH: the smaller the number of small aerosol particles, the larger the effective radius and the smaller the Angstrom coefficient. The hygroscopic growth behaviors and the coarse nature of the marine tropical aerosols reveal an immense potential of light scattering enhancement at longer wavelength and at high humidities and the potential for being highly effective cloud condensation nuclei.

About the two formulas used for the computations of the effective refractive indices, it can be concluded that they are the same, because they gave almost similar plots at the same computational platform that is, they display the same information. They show that refractive index is highly variable depending on the chemical compositions of aerosols and the type of the mixing state (d'Almeida et al., 1991).

Finally, the data fitted our models very well and can be used to extrapolate the hygroscopic growth at any RH and enhancement parameters at any RH and wavelengths. The importance of determining $gf_{mix}(RH)$ as a function of RH and volume fractions, mass fractions and number fractions, and enhancement parameters as a function of RH and wavelengths can be potentially important because it can be used for efficiently representing aerosols-water interactions in global models.

REFERENCES

Andreae, M. O. and Rosenfeld, D.: Aerosol-cloud-precipitation interactions, Part 1, The nature and sources of cloud-active aerosols, Earth-Sci. Rev., 89, 13–41, 2008.

Angstrom, A.(1961): Techniques of Determining the Turbidity of the At-mosphere, Tellus, 13, 214–223,.

Aspens D. E. (1982), Local-field effect and effective medium theory: A microscopic perspective Am. J. Phys. 50, 704-709.

Berg, H. O., Swietlicki, E., and Krejci, R.: Hygroscopic growth of aerosol particles in the marine boundary layer over the Pacific and Southern Oceans during the First Aerosol Characterization Experiment (ACE 1), J. Geophys. Res., 103, 16 535–16 545, 1998.

Birmili, W., Nowak, A., Schwirn, K., Lehmann, K.et al. (2004) A new method to accurately relate dry and humidified number size distributions of atmospheric aerosols. Journal of Aerosol Science 1, 15–16, Abstracts of EAC, Budapest 2004.

Cheng, Y. F., Wiedensohler, A., Eichler, H., Heintzenberg, J., Tesche, M., Ansmann, A., Wendisch, M., Su, H., Althausen, D., Herrmann, H., Gnauk, T., Br¨ uggemann, E., Hu, M., and Zhang, Y. H.: Relative humidity dependence of aerosol optical properties and direct radiative forcing in the surface boundary layer at Xinken in Pearl River Delta of China: An observation based numerical study, Atmos. Environ., 42, 6373–6397, 2008.

Christensen, S. I. and Petters, M. D. (2012). Th e role of temperature in cloud droplet activation. J. Phys. Chem. A 116(39): 9706–9717.

Chylek, P., and J. Wong (1995), Effect of absorbing aerosols on global radiation bud get, Geophys . Res. Lett. , 22(8), 929 – 931, doi: 10.1 029/95GL00800.

Clarke, A., et al. (2007), Biomass burning and pollution aerosol over North America: Organic components and their influence on spectral optical properties and humidification response, J. Geophys. Res., 11 2, D12S18, doi:10.1029/2006JD007777.

d'Almeida, G. A., P. Koepke, and E. P. Shettle (1991),Atmospheric Aerosols: Global Climatology and Radiative Characteristics, 561 pp., A. Deepak, Hampton, Va

Doherty, et al., (2005). A comparison and summary of aerosol optical properties as observed in situ from aircraft, ship, and land during ACE-Asia. Journal of Geophysical Research 110, D04201.

Duplissy J., P. F. DeCarlo, J. Dommen, M. R. Alfarra, A. Metzger, I. Barmpadimos, A. S. H. Prevot, E. Weingartner, T. Tritscher, M. Gysel, A. C. Aiken, J. L. Jimenez, M. R. Canagaratna , D. R. Worsnop, D. R. Collins, J. Tomlinson, and U. Baltensperger, Relating hygroscopicity and composition of organic aerosol particulate matter Atmos. Chem. Phys., 11, 1155–1165, 2011 www.atmos-chem-phys.net/11/1155/2011/ doi:10.5194/acp-11-1155-2011.

Eck, T. F., Holben, B. N., Dubovic, O., Smirnov, A., Slutsker, I., Lobert, J. M., and Ramanathan, V.: Column-integrated aerosol optical properties over the Maldives during the northeast mon-soon for 1998–2000, J. Geophys. Res., 106, 28 555–28 566, 2001.

Eck, T. F., Holben, B. N., Reid, J. S., Dubovic, O., Smirnov, A., O'Neil, N. T., Slutsker, I., and Kinne, S.: Wavelength dependence of the optical depth of biomass burning, urban, and desert dust aerosols, J. Geophys. Res., 104(D24), 31 333–31 349, 1999.

Eck, T. F., Holben, B. N., Ward, D. E., Dubovic, O., Reid, J. S., Smirnov, A., Mukelabai, M. M., Hsu, N. C., O' Neil, N. T., and Slutsker, I.: Characterization of the optical properties of biomass burning aerosols in Zambia during the 1997 ZIBBEE field campaign, J. Geophys. Res., 106(D4), 3425–3448, 2001.

Fierz-Schmidhauser, R., Zieger, P., Gysel, M., Kammermann, L., DeCarlo, P. F., Baltensperger, U., and Weingartner, E.: Measured and predicted aerosol light scattering enhancement factors at the high alpine site Jungfraujoch, Atmos. Chem. Phys., 10, 2319–2333, doi:10.5194/acp-10-2319-2010, 2010b

Fierz-Schmidhauser, R., Zieger, P., Vaishya, A., Monahan, C., Bialek, J., O'Dowd, C. D., Jennings, S. G., Baltensperger, U., and Weingartner, E.: Light scattering enhancement factors in the marine boundary layer (Mace Head, Ireland), J. Geophys. Res., 115, D20204, doi:10.1029/2009JD013755, 2010a.

Fitzgerald, J. W. (1975) Approximation formulas for the equilibrium size of an aerosol particle as a function of its dry size and composition and ambient relative humidity. J. Appl. Meteorol., 14, 1044 –1049

Gasso S., et al. (2000), Influence of humidity on the aerosol scattering coefficient and its effect on the upwelling radiance during ACE-2, Tellus, Ser. B , 52, 546 – 567.

Gunthe, S. S., King, S. M., Rose, D., Chen, Q., Roldin, P., Farmer, D. K., Jimenez, J. L., Artaxo, P., Andreae, M. O., Martin, S. T., and Poschl, U.: Cloud condensation nuclei in pristine tropical rainforest air of Amazonia: size-resolved measurements and modeling of atmospheric aerosol composition and CCN activity, Atmos. Chem. Phys., 9, 7551–7575, doi:10.5194/acp-9-7551-2009, 2009.

Gysel, M., McFiggans, G. B., and Coe, H.: Inversion of tandem differential mobility analyser (TDMA) measurements, J. Aerosol Sci., 40, 134–151, 2009.

Hanel, G. (1976). The Properties of Atmospheric Aerosol Particles as Functions of Relative Humidity at Thermodynamic Equilibrium with Surrounding Moist Air. In Advances in Geophysics, Vol. 19 , H. E. Landsberg and J. Van Mieghem, eds., Academic Press, New York, pp. 73–188.

Heller, W. (1945), The determination of refractive index of colloidal particles by means of a new mixture rule or from measurements of light scattering,Phys. Rev., 68, 5 – 10.

Hess M., Koepke P., and Schult I (May 1998), Optical Properties of Aerosols and Clouds: The Software Package OPAC, Bulletin of the American Met. Soc. 79, 5, p831-844.

Jacobson, M. Z.: Strong radiative heating due to the mixing state of black carbon in atmospheric aerosols, Nature, 409, 695–697, 2001.

Jeong M. J, Li Z., Andrews E., Tsay S. C., (2007) Effect of aerosol humidification on the column aerosol optical thickness over the Atmospheric Radiation Measurement Southern Great Plains site, J. Geophys. Res., 112, D10202, doi:10.1029/2006JD007176.

Kammermann, L., Gysel, M., Weingartner, E., and Baltensperger, U.: 13-month climatology of the aerosol hygroscopicity at the free tropospheric site Jungfraujoch (3580 m a.s.l.), Atmos. Chem. Phys., 10, 10717–10732, doi:10.5194/acp-10-10717-2010, 2010.

Kaskaoutis, D. G. and Kambezidis, H. D.(2006): Investigation on the wavelength dependence of the aerosol optical depth in the Athens area, Q. J. R. Meteorol. Soc., 132, 2217–2234,.

Kasten, F.: Visibility forecast in the phase of pre-condensation, Tel-lus, XXI, 5, 631–635, 1969.

Kaufman, Y. J. (1993), Aerosol optical thickness and atmospheric path radiance, J. Geophys. Res., 98, 2677-2992.

Kim, J., Yoon,, S.-C., Jefferson, A., and Kim, S.-W.: Aerosol hygroscopic properties during Asian dust, pollution, and biomass burning episodes at Gosan, Korea in April 2001, Atmos. Environ., 40, 1550–1560, 2006.

King, M. D. and Byrne, D. M.(1976): A method for inferring total ozone content from spectral variation of total optical depth obtained with a solar radiometer, J. Atmos. Sci., 33, 2242–2251.

Kohler, H.: The nucleus and growth of hygroscopic droplets, Trans. Faraday Soc., 32, 1152–1161, 1936.

Kuśmierczyk-Michulec, J. (2009). Ångström coefficient as an indicator of the atmospheric aerosol type for a well- mixed atmospheric boundary layer: Part 1: Model development. Oceanologia , Vol. 51, p. 5-39.

Latha, M.K., Badarinath, K.V.S., (2005). Factors influencing aerosol characteristics over urban environment. Environmental Monitoring and Assessment 104, 269–280.

Liou, K. N. (2002), An Introduction ro Atmospheric Radiation, 583pp., Elsevier, New York.

Liu P. F., Zhao C. S., Gobel T., Hallbauer E., Nowak A., Ran L., Xu W. Y., Deng Z. Z., Ma N., Mildenberger K., Henning S., Stratmann F., and Wiedensohler A. (2011) Hygroscopic proper ties of aerosol par ticles at high relative humidity and their diurnal variations in the Nor th China Plain, Atmos. Chem. Phys. Discuss., 11, 2991–3040

Lorentz, H. A. (1880). Ueber die Beziehung zwischen der Fortpflanzungsgesch windigkeit des Lichtes und der Korperdichte. Ann. P hys. Chem. 9, 641–665.

Lorenz, L. (1880). Ueber die Refractionconstante. A nn. P hys. Chem. 11, 70–103.

Martin, S. T., Hung, H. M., Park, R. J., Jacob, D. J., Spurr, R. J. D., Chance, K. V., and Chin, M.: Effects of the physical state of tropospheric ammonium-sulfate-nitrate particles on global aerosol direct radiative forcing, Atmos. Chem. Phys., 4, 183–214, 2004, SRef-ID: 1680-7324/acp/2004-4-183.

Martinez-Lozano, J.A., Utrillas, M.P., Tena, F., Pedros, R., Canada, J., Bosca, J.V., Lorente, J., (2001). Aerosol optical characteristics from summer campaign in an urban coastal Mediterranean area. IEEE Transactions on Geoscience and Remote Sensing 39, 1573–1585.

Massling A., S. Leinert, A. Wiedensohler, and D. Covert (2006) Hygroscopic growth of sub-micrometer and one-micrometer aerosol particles measured during ACE-Asia, Atmos. Chem. Phys. Discuss., 6, 12267–12300, 2006 www.atmos-chem-phys-discuss.net/6/12267/2006/

Massling, A., Wiedensohler, A., Busch, B., Neusuß, C., Quinn, P., Bates, T., and Covert, D.: Hygroscopic properties of different aerosol types over the Atlantic and Indian Oceans, Atmos. Chem. Phys., 3, 1377–1397, 2003.

Meier J., B. Wehner, A. Massling, W. Birmili, A. Nowak, T. Gnauk, E. Br¨ uggemann, H. Herrmann, H. Min, and A. Wiedensohler Hygroscopic growth of urban aerosol particles in

Beijing (China) during wintertime: a comparison of three experimental methods, Atmos. Chem. Phys., 9, 6865–6880, 2009 www.atmos-chem-phys.net/9/6865/2009/

Moffet, R. C. and Prather, K. A.: In-situ measurements of the mixing state and optical properties of soot with implications for radiative forcing estimates, P. Natl. Acad. Sci. USA, 106, 11872–11877, doi:10.1073/pnas.0900040106, 2009.

Niedermeier, D., Wex, H., Voigtl¨ ander, J., Stratmann, F., Br ¨ uggemann, E., Kiselev, A., Henk, H., and Heintzenberg, J.: LACIS-measurements and parameterization of sea-salt particle hygroscopic growth and activation, Atmos. Chem. Phys., 8, 579–590, doi:10.5194/acp-8-579-2008, 2008.

O'Neill, N. T., Dubovic, O., and Eck, T. F.(2001): Modified Angstrom exponent for the characterization of submicrometer aerosols, Appl. Opt., 40(15), 2368–2375.

O'Neill, N. T., Eck, T. F., Smirnov, A., Holben, B. N., and Thulasiraman, S.: Spectral discrimination of coarse and fine mode optical depth, J. Geophys. Res., 198(D17), 4559, doi:101029/2002JD002975, 2003.

Ogren, J. A. and Charlson R. J.: Implications for models and measurements of chemical inhomogeneities among cloud droplets, Tellus, 44B, 489–504, 1992.

Orr Jr. C., Hurd F. K., Corbett W. J., 1958, Aerosol size and relative humidity, J. Colloid Sci., 13, 472–482.

Oshima, N., Koike, M., Zhang, Y., Kondo, Y., Moteki, N., Takegawa, N., and Miyazaki, Y.: Aging of black carbon in outflow from anthropogenic sources using a mixing state resolved model: Model development and evaluation, J. Geophys. Res., 114, D06210, doi:10.1029/2008jd010680, 2009.

Pahlow, M., Feingold, G., Jefferson, A., Andrews, E., Ogren, J. A., Wang, J., Lee, Y.-N., Ferrare, R. A., and Turner, D. D.: Comparison between lidar and nephelometer measurements of aerosol hygroscopicity at the Southern Great Plains Atmospheric Radiation Measurement site, J. Geophys. Res., 111, D005S15, doi:10.1029/2004JD005646, 2006.

Pedros, R., Martinez-Lozano, J. A., Utrillas, M. P., Gomez-Amo, J. L., and Tena, F.(2003): Column-integrated aerosol, optical properties from ground-based spectroradiometer measurements at Barrax (Spain) during the Digital Airborne Imaging Spectrometer Experiment (DAISEX) campaigns, J. Geophys. Res., 108(D18), 4571, doi:10.1029/2002JD003331.

Penner, J. E., Dickinson, R. E. and O'Neil, C. A. (1992). Effects of aerosol from biomass burning on the global radiation budget. Science, 256, 1432-1434.

Petters, M. D. and Kreidenweis, S. M. (2007). A single parameter representation of hygroscopic growth and cloud condens ation nucleus activity. Atmos. Chem. Phys. 7(8): 1961–1971.

Petters, M. D., Wex, H., Carrico, C. M., Hallbauer, E., Massling, A., McMeeking, G. R., Poulain, L., Wu, Z., Kreidenweis, S. M., and Stratmann, F.: Towards closing the gap between hygroscopic growth and activation for secondary organic aerosol: Part 2 theoretical approaches, Atmos. Chem. Phys., 9, 3999–4009, doi:10.5194/acp-9-3999-2009, 2009.

Poschl, U., Rose, D., and Andreae, M. O.: Climatologies of cloudrelated aerosols – part 2: Particle hygroscopicity and cloud condensation nuclei activity, in: Clouds in the perturbed climate system, edited by: Heintzenberg, J. and Charlson, R. J., MIT Press, Cambridge, 2009.

Putaud, J.-P.: Interactive comment on "Aerosol hygroscopicity at Ispra EMEP-GAW station" by M. Adam et al., Atmos. Chem. Phys. Discuss., 12, C1316–C1322, 2012.

Quinn, P. K., et al. (2005) , Impact of particulate organic matter on the relative humidity dependence of light scattering: A simplified parameterization, Geophys. Res. Lett., 32, L22809, doi:10.1029/2005GL024322.

Randles , C. A. , Russell L. M. and. Ramaswamy V. (2004) Hygroscopic and optical properties of organic sea salt aerosol and consequences for climate forcing, Geophysical Research Letters, Vol. 31, L16108, doi:10.1029/2004GL020628.

Riemer, N., West, M., Zaveri, R. A., and Easter, R. C.: Simulating the evolution of soot mixing state with a particleresolved aerosol model, J. Geophys. Res., 114, D09202, doi:10.1029/2008jd011073, 2009.

Riemer, N., West, M., Zaveri, R., and Easter, R.: Estimating black carbon aging time-scales with a particle-resolved aerosol model, J. Aerosol Sci., 41, 143–158, 2010.

Rissler, J., Svenningsson, B., Fors, E. O., Bilde, M., and Swietlicki, E.: An evaluation and comparison of cloud condensation nucleus activity models: Predicting particle critical saturation from growth at subsaturation, J. Geophys. Res., 115, D22208, doi:10.1029/2010jd014391, 2010.

Rose, D., Gunthe, S. S., Mikhailov, E., Frank, G. P., Dusek, U., Andreae, M. O., and P¨ oschl, U.: Calibration and measurement uncertainties of a continuous-flow cloud condensation nuclei counter (DMT-CCNC): CCN activation of ammonium sulfate and sodium chloride aerosol particles in theory and experiment, Atmos. Chem. Phys., 8, 1153–1179, doi:10.5194/acp-8-1153-2008, 2008.

Schmid, B., Hegg, D.A., Wang, J., Bates, D., Redemann, J., Russell, P.B., Livingston, J.M., Jonsson, H.H., Welton, E.J., Seinfeld, J.H., Flagan, R.C., Covert, D.S., Dubovik, O., Jefferson, A., (2003). Column closure studies of lower tropospheric aerosol and water vapor during ACE-Asia using airborne Sun photometer and airborne in situ and ship-based lidar measurements. Journal of Geophysical Research 108 (D23), 8656.

Schmidhauser, R., Zieger, P., Weingartner, E., Gysel, M., DeCarlo, P. F., and Baltensperger, U: Aerosol light scattering at high relative humidity at a high alpine site (Jungfraujoch), European Aerosol Conference, Karlsruhe, Germany, 6–11 September 2009, T047A07, 2009.

Schuster, G.L., Dubovik, O. and Holben, B.N. (2006). Angstrom Exponent and Bimodla Aerosol Size Distributions. J. Geophy. Res. 111: 7207.

Segan, C. and Pollack, J. (1967). Anisotropic nonconservative scattering and the clouds of Venus. J. Geophys. Res. 72, 469-477.

Seinfeld, J. and Pandis, S. N. (2006): Atmospheric Chemistry and Physics, Wiley-Interscience, New York, NY, USA, 2nd edn.

Seinfeld, J. H. and Pandis, S. N.(1998): Atmospheric Chemistry and Physics, Wiley-Interscience publication.

Shettle, E. P., and R. W. Fenn (1979), Models for the aerosols of the lower atmosphere and the effects of humidity variations on their optical properties, Rep. no. AFGL-TR-79-0214, ERP No. 676,AirForceGeophys. Lab., Optical Phys. Div., Hanscom Air Force Base, Mass.

Sjogren, S., Gysel, M., Weingartner, E., Baltensperger, U., Cubi-son, M. J., Coe, H., Zardini, A. A., Marcolli, C., Krieger, U. K., and Peter, T.(2007): Hygroscopic growth and water uptake kinetics of two-phase aerosol particles consisting of ammonium sulfate, adipic and humic acid mixtures, J. Aerosol Sci., 38, 157–171, doi:10.1016/j.jaerosci.2006.11.005.

Stock M., Y. F. Cheng, W. Birmili, A. Massling, B. Wehner, T. Muller, S. Leinert, N. Kalivitis,N. Mihalopoulos, and A. Wiedensohler, (2011) Hygroscopic properties of atmospheric aerosol

particles over the Eastern Mediterranean: implications for regional direct radiative forcing under clean and polluted conditions, Atmos. Chem. Phys., 11, 4251–4271, www.atmos-chem-phys.net/11/4251/2011/ doi:10.5194/acp-11-4251-2011

Stokes, R. H. and Robinson, R. A. (1966): Interactions in aqueous nonelec-trolyte solutions. I. Solute-solvent equilibria, J. Phys. Chem., 70, 2126–2130.

Sullivan, R. C., Moore, M. J. K., Petters, M. D., Kreidenweis, S. M., Roberts, G. C., and Prather, K. A.: Effect of chemical mixing state on the hygroscopicity and cloud nucleation properties of calcium mineral dust particles, Atmos. Chem. Phys., 9, 3303–3316, doi:10.5194/acp-9-3303-2009, 2009.

Swietlicki, E., Hansson, H., Hameri, K., Svenningsson, B., Massling, A., McFiggans, G., McMurry, P., Petaja, T., Tunved, P., Gysel, M., et al.: Hygroscopic properties of submicrometer atmospheric aerosol particles measured with H-TDMA instruments in various environments -A review, Tellus B, 60, 432-469, 2008.

Swietlicki, E., Hansson, H.-C., H¨ ameri, K., Svenningsson, B., Massling, A., McFiggans, G., McMurry, P. H., Pet¨ aj ¨ a, T., Tunved, P., Gysel, M., Topping, D., Weingartner, E., Baltensperger, U., Rissler, J., Wiedensohler, A., and Kulmala, M.: Hygroscopic properties of submicrometer atmospheric aerosol particles measured with H-TDMA instruments in various environments: a review, Tellus B, 60, 432–469, 2008

Swietlicki, E., Zhou, J. C., Covert, D. S., Hameri, K., Busch, B., Vakeva, M., Dusek, U., Berg, O. H., Wiedensohler, A., Aalto, P., Makela, J., Martinsson, B. G., Papaspiropoulos, G., Mentes, B., Frank, G., and Stratmann, F.(2000): Hygroscopic properties of aerosol particles in the northeastern Atlantic during ACE-2, Tellus, 52B, 201–227.

Tang I. N., (1976), Phase transformation and growth of aerosol particles composed of mixed salts, J. Aerosol Sci., 7, 361–371.

Tang, I. N. (1996) Chemical and size effects of hygroscopic aerosols on light scattering coeffcients. J. Geophys . R es. , 101, 19245 – 19250

Topping, D. O., McFiggans, G. B., and Coe, H.: A curved multi-component aerosol hygroscopicity model framework: Part 1-Inorganic compounds, Atmos. Chem. Phys., 5, 1205-1222, doi:10.5194/acp-5-1205-2005, 2005a

Topping, D. O., McFiggans, G. B., and Coe, H.: A curved multicomponent aerosol hygroscopicity model framework: Part 2-Including organic compounds, Atmos. Chem. Phys., 5, 1223-1242, doi:10.5194/acp-5-1223-2005, 2005b.

Twomey, S.: Atmospheric aerosols, Elsevier, New York, 1977.

Wang J. and Martin S. T. (2007) Satellite characterization of urban aerosols: Importance of including hygroscopicity and mixing state in the retrieval algorithms, Journal Of Geophysical Research, Vol. 112, D17203, doi:10.1029/2006JD008078.

Wang J., and Martin S. T. (2007), Satellite characterization of urban aerosols: Importance of including hygroscopicity and mixing state in the retrieval algorithms, J. Geophys. Res., 112 , D 17203, doi:1 0.1029 /2006JD008078.

Wex, H., Hennig, T., Salma, I., Ocskay, R., Kiselev, A., Henning, S., Massling, A., Wiedensohler, A., and Stratmann, F.: Hygroscopic growth and measured and modeled critical super-saturations of an atmospheric HULIS sample, Geophys. Res. Lett., 34, L02818, doi:10.1029/2006gl028260, 2007.

Whitby, K. (1978), The physical characteristics of sulfur aerosols, Atmos. Environ., 12, 135–159.

Zhang, R., Khalizov, A. F., Pagels, J., Zhang, D., Xue, H., and McMurry, P. H.: Variability in morphology, hygroscopicity, and optical properties of soot aerosols during atmospheric processing, P. Natl. Acad. Sci. USA, 105, 10291–10296, 2008.

Zieger, P., Weingartner, E., Henzing, J., Moerman, M., de Leeuw, G., Mikkil¨ a, J., Ehn, M., Pet ¨ aj ¨ a, T., Cl ´ emer, K., van Roozendael, M., Yilmaz, S., Frieß, U., Irie, H., Wagner, T., Shaiganfar, R., Beirle, S., Apituley, A., Wilson, K., and Baltensperger, U.: Comparison of ambient aerosol extinction coefficients obtained from in-situ, MAX-DOAS and LIDAR measurements at Cabauw, Atmos. Chem. Phys., 11, 2603–2624, doi:10.5194/acp-11-2603-2011, 2011.